Korean J. Chem. Eng., **28**(2), 591-596 (2011)
DOI: 10.1007/s11814-010-0467-1

Separation of tetrahydrofuran and water using pressure swing distillation: Modeling and optimization

Jihwan Lee*, Jungho Cho,†, Dong Min Kim***, and Sangjin Park***

*Department of Chemical Engineering, Dongguk University, 26, Pil-dong 3-ga, Jung-gu, Seoul 100-715, Korea
**Department of Chemical Engineering, Kongju National University, 275, Budae-dong, Cheonan, Chungnam 330-717, Korea
***Department of Materials Science and Engineering, Hongik University, 300, Shian, Yongi, Chungnam 339-701, Korea
(*Received 6 July 2010 • accepted 27 October 2010*)

Abstract−Computer simulations were performed to obtain highly pure tetrahydrofuran (THF) with over 99.9 mole% from the mixture of THF and water. Pressure swing distillation (PSD) was used since the azeotropic point between tetrahydrofuran and water can be varied with pressure. A commercial process simulator, PRO/II with PROVISION release 8.3, was used for the simulation studies. The Wilson liquid activity coefficient model was used to simulate the low pressure column, and the Peng-Robinson equation of state model was added to correct the vapor phase non-idealities for the modeling of the high pressure column. The most optimal reflux ratios and the most optimal feed stage locations that could minimize the total reboiler heat duties were determined.

Key words: Pressure Swing Distillation, Tetrahydrofuran, Computer Simulation, Liquid Activity Coefficient Mode, Equation of State

INTRODUCTION

Distillation, the most frequently used separation method in chemical processes, is based on the difference in the relative volatilities of the components of a liquid mixture [1]. PSD has often been mentioned as an alternative process to the distillation process [2] that can separate the two components that form azeotrope. The PSD is based on the principle that the azeotropic composition can vary considerably by changing the pressure, which will make separation easier. The pressure sensitivity of azeotropes has been known since the 1860s [3,4]. Lewis [5] was the first to exploit this property of distilling azeotropic mixtures. The PSD process can be environmentally acceptable since it does not require any other separating agents. However, azeotropic distillation normally uses an entrainer, which is a volatile organic compound that can be harmful to the environment. Knapp and Doherty [2] listed 36 pressure-sensitive binary azeotropes as examples. The most complete collection of the azeotropic data was published by Gmehling et al. [6].

Batch distillation is an important part of high-purity chemical production. It is an important process in the pharmaceutical and several other industries such as the treatment of waste solvent mixtures. Recently, several authors investigated the pressure swing distillation in batch [7-11] and in continuous mode [12-14]. The batch PSD was first studied experimentally by Repke et al. [7]. Modla et al. studied the batch PSD by feasibility studies and rigorous simulation and proposed new configurations [9]. Luyben compared the continuous extractive distillation and PSD for the separation of the mixture acetone-methanol [13].

Phimister and Seider [15] studied the separation of THF-water azeotropic system by semi-continuous PSD and reverse-batch operation. It was found that the semicontinuous column achieved better performance than the batch stripper. They also compared their performance with that of a continuous system. The separation of highly volatile organics, such as THF, is industrially important since the aqueous solution of THF appears in many chemical processes [16]. The objective of this study is a computational analysis of the PSD process in order to separate the binary mixture of THF and water by computer simulations and optimizations using PRO/II with PROVISION release 8.3.

Table 1 summarizes binary azeotropic systems that can be separated by PSD [2]. In addition to the PSD process, there are several separation methods. For instance, the isopropanol and water binary mixture can be separated by an extractive distillation process that uses triethylene glycol solvent. The ethanol and water binary azeotropic mixture can be separated by an azeotropic distillation process that uses benzene or cyclohexane as an entrainer [17,18]. Since

Table 1. Examples of binary azeotropes

No.	Components
1	Carbon dioxide - ethylene
2	Hydrochloric acid - water
3	Water - acetonitrile
4	Water - ethanol
5	Water - acrylic acid
6	Water - acetone
7	Water - propylene oxide
8	Water - methyl acetate
9	Water - propionic acid
10	Water - 2-methoxyethanol
11	Water - 2-butanol (Methyl Ethyl Ketone (MEK))
12	Water - tetrahydrofuran (THF)

†To whom correspondence should be addressed.
E-mail: jhcho@kongju.ac.kr

the azeotropic point between ethanol and water disappears under 11.5 kPa, simple distillation can be applied to separate them into each pure component. However, since this case requires a vacuum system, the diameter of the distillation column increases due to the reduced density in the vapor phase. Moreover, due to the decreased temperature of the top product, a refrigeration system is needed to cool the cooling agent, which requires a lower temperature than the cooling water. The azeotropic distillation process and the extractive distillation process require an entrainer or a solvent as an additional agent. Hence, the PSD process is an eco-friendly process because this process does not require any additional separating agent, entrainer, or solvent.

Fig. 1 shows the equilibrium diagram for THF and water at 1 bar and 7 bar, respectively. The solid line in the graph is the vapor-liquid equilibrium diagram for the THF and water at 1 bar. The dotted line is the vapor-liquid phase equilibrium at a high pressure, 7 bar.

Fig. 2 shows a schematic diagram for the PSD process between THF and water. THF can be widely used as a solvent for many resins, printing inks, and extraction, etc. The THF-water binary mixture, Point E in Fig. 1, is fed to the middle stage of the H_2O removal column, T01. Since this column operates around an atmospheric pressure, the composition distribution follows the solid line. The objective of this column is to concentrate the THF near an azeotropic point between THF and water and to remove water as a column bottom stream. At the top of the H_2O removal column, the feed mixture is concentrated to the point of just before the azeotropic point between THF and water at 1 bar (Point A). At the bottom of the column, nearly pure water is obtained (Point B). If the top product stream of the first column is pressurized to 7 bar simply by pumping, the vapor-liquid equilibrium between THF and water follows the dotted line shown in Fig. 1 and the relative volatility between THF and water is reversed. The top stream of the first column feeds to the mid-stage of the THF recovery column, T02. The top stream of the THF recovery column near the azeotropic point between THF and water is obtained at 7 bar around a point C and this is recycled to mix with the feed stream. On the other hand, nearly pure THF (Point D) can be produced at the bottom stream of the THF recovery column.

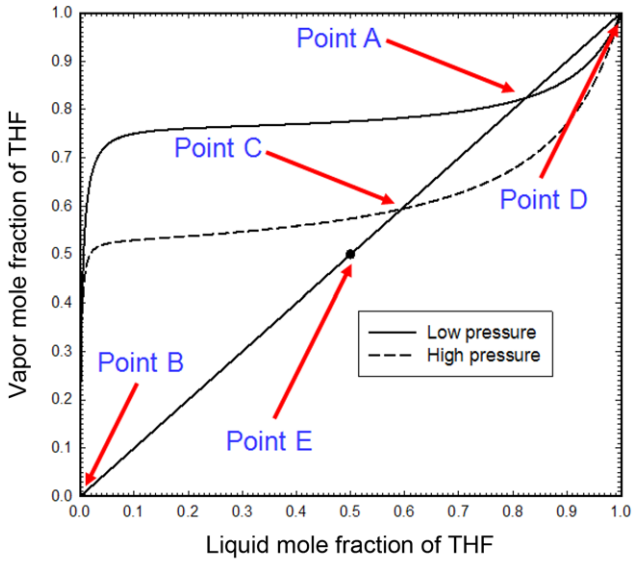

Fig. 1. Vapor-liquid equilibria for THF and water at 1 bar and 7 bar, respectively.

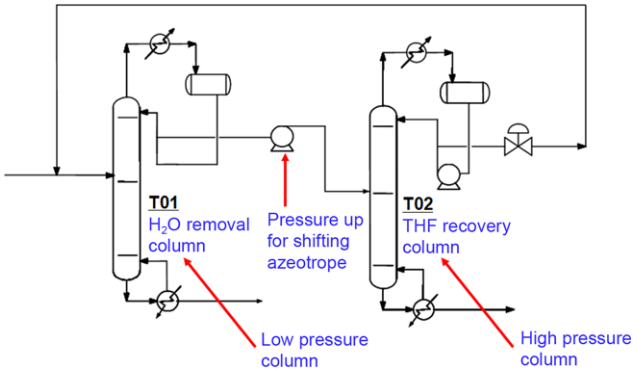

Fig. 2. A schematic diagram of the pressure swing distillation process for THF and water binary system.

THERMODYNAMIC THEORY

In general, vapor-liquid equilibrium calculations can be divided into two types. The starting point for both is the equality of fugacities of a component 'i' in the vapor and liquid phases, as shown in Eq. (1). The two types differ in the description of the component fugacities in the vapor and liquid phases.

$$\hat{f}_i^v(T,P,y_i) = \hat{f}_i^l(T,P,x_i) \tag{1}$$

The correlations of the first types involve a "two-model" approach: one model is used to estimate the vapor phase non-idealities while another model is used for the liquid phase. The starting equations are:

$$\hat{f}_i^v(T,P,y_i) = \hat{\phi}_i^l y_i P \quad \text{for vapor phase} \tag{2a}$$

$$\hat{f}_i^l(T,P,x_i) = \gamma_i x_i P_i^{vap} \quad \text{for liquid phase} \tag{2b}$$

A typical example of the two-model approach is to use an equation of state, such as the Soave-Redlich-Kwong [19] or Peng-Robinson [20] model to estimate the vapor phase fugacity coefficient and liquid activity coefficient model such as the Wilson [21-23] or NRTL [24] model.

Since the operating pressure of the first column in the PSD process is only 1 bar, the vapor phase can be regarded as ideal. Therefore, $\hat{\phi}_i^v$ is equal to 1 since the vapor phase can be assumed to be ideal. Because the operating pressure of the second column is 7 bar, the Peng-Robinson equation of state was used to estimate the vapor phase non-idealities, as shown in Eq. (3).

$$P = \frac{RT}{v-b} - \frac{a_c \alpha}{v(v+b)+b(v-b)} \tag{3}$$

To estimate the activity coefficient of component 'i', the liquid activity coefficient model suggested by Wilson was used as shown in Eqs. (4) and (5).

$$\ln \gamma_i = 1 - \ln \sum_{j=1}^{N} x_j A_{ij} - \sum_{k=1}^{N} \frac{x_i A_{ki}}{\sum_{j=1}^{N} x_j A_{kj}} \tag{4}$$

Table 2. Wilson binary interaction parameters

Component i	Component j	a_{ij}	a_{ji}
THF	Water	4,150.7192	795.4237

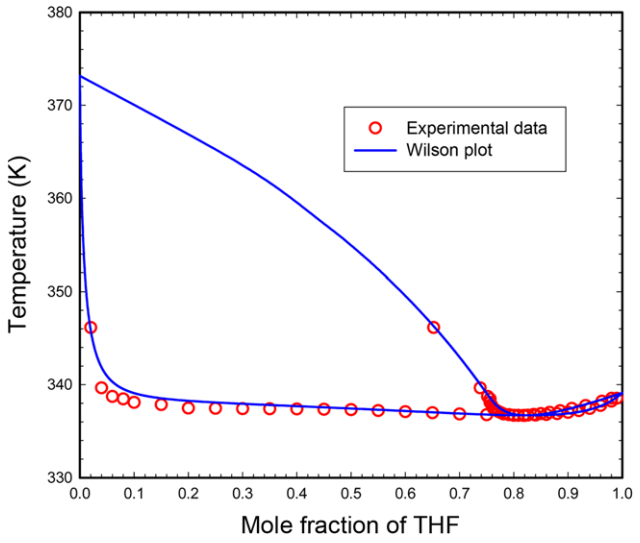

Fig. 3. Isobaric experimental data of THF and water mixture at 1.013 bar and its prediction with the Wilson model.

$$A_{ij} = \frac{v_j^L}{v_i^L} \exp\left(-\frac{a_{ij}}{T}\right) \quad (5)$$

In Eq. (5), T represents the absolute temperature. There are also two binary interaction parameters, a_{ij} and a_{ji}, for each binary component shown in Eq. (5). The binary interaction parameters of the Wilson model were determined by regressing the experimental vapor-liquid equilibrium data for the THF and water system, where the pattern search algorithm suggested by Nelder and Mead [25] was used to determine the optimal binary interaction parameters. The Wilson binary interaction parameters are shown in Table 2. The objective function of the thermodynamic data regression was defined, as shown in Eq. (6).

$$\text{Objective} = \sum_{j=1}^{N} \left(\frac{T_j^{exp} - T_j^{cal}}{T_j^{exp}}\right)^2 \quad (6)$$

Fig. 3 shows a comparison between the binary isobaric vapor-liquid phase equilibrium data and the predicted results by using the Wilson model for the THF and water system.

SIMULATION OF THE THF RECOVERY DISTILLATION PROCESS AND OPTIMIZATION

The feed conditions for the THF recovery system by the PSD process are summarized in Table 3.

The first step for the simulation of the PSD process is to determine the operating pressures of the lower and higher columns, respectively [26]. Fig. 4 shows a diagram of the THF mole fraction and the temperature of the azeotrope between THF and water with pressure. The cold utility is cooling water with a supply temperature of 32 °C and a return temperature of 40 °C. Therefore, the operating temperature of the overhead reflux drum fixed at 45 °C. The

Table 3. Feedstock information

Component	Flowrate (kmol/h)
THF	50.0
Water	50.0
Total flow	100.0
Temperature (°C)	25.0
Pressure (bar)	2.5

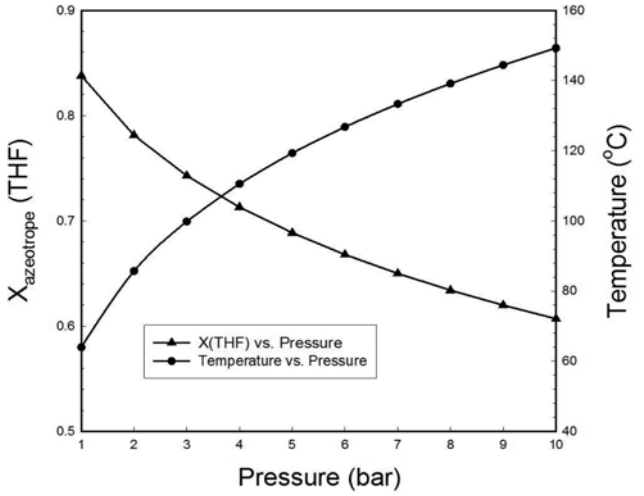

Fig. 4. THF mole fraction and temperature of the azeotrope as a function of pressure.

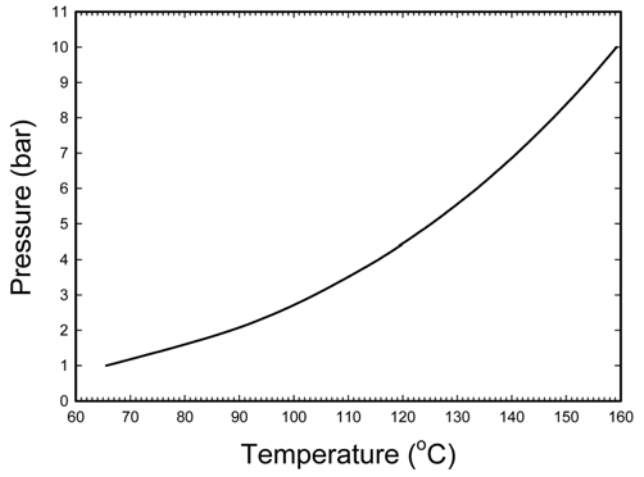

Fig. 5. Vapor pressure of THF as a function of temperature.

operating pressure of the H_2O removal column was selected within a temperature range that cooling water can be used as a cooling medium for the overhead condenser. Fig. 5 shows the vapor pressure of the THF plotted as a function of temperature. The operating pressure of the THF recovery column was 7 bar, considering that the temperature difference was 40 °C between column bottom temperature, 140 °C, and steam temperature, 180 °C.

The design conditions for each column are summarized in Table 4. As shown, the theoretical stages of each distillation column were fixed to 25 stages, including a condenser and a reboiler. The operat-

Table 4. Design conditions for each column

Column	H_2O removal column	THF recovery column
Theoretical stage number	25	25
Reflux ratio	Manipulated	Manipulated
Feed stage location from top	12	4
Condenser type	Sub-cooled	Sub-cooled
Condenser temperature	45 °C	45 °C
Cooling water supply temperature	32 °C	32 °C
Cooling water return temperature	40 °C	40 °C
Steam condition	180 °C Saturated	180 °C Saturated
Condenser pressure	1.05 bar	7.00 bar
Column top pressure	1.2 bar	7.2 bar
Column pressure drop	0.3 bar	0.3 bar
Internal type	Valve tray	Valve tray
THF mole%	0.01	99.9
H_2O mole%	99.0	0.01

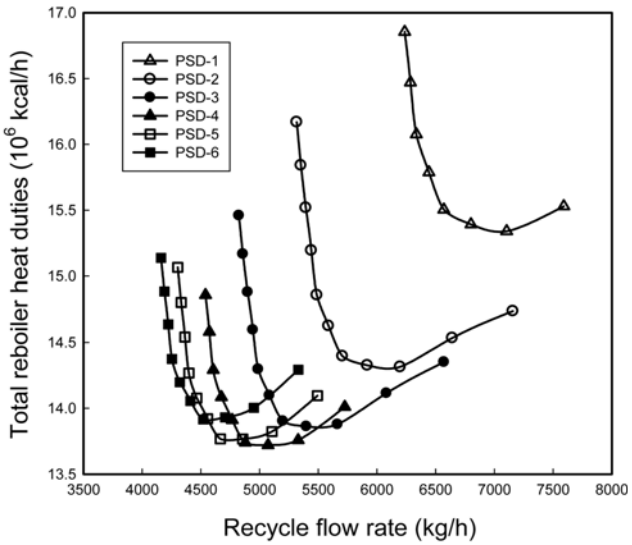

Fig. 6. Total reboiler heat duties versus recycle flow rate in the pressure swing distillation process.

Table 5. Minimized total reboiler heat duties for each reflux ratio of the T01 column

Case	T01 column reflux ratio	Recycle flow rate (kg/h)	Total reboiler heat duties (10^6 kJ/h)
Case 1	0.1	6,800.7	15.3919
Case 2	0.2	6,196.9	14.3149
Case 3	0.3	5,399.0	13.8625
Case 4	0.4	5,072.5	13.7209
Case 5	0.5	4,855.8	13.7672
Case 6	0.6	4,706.3	13.9308

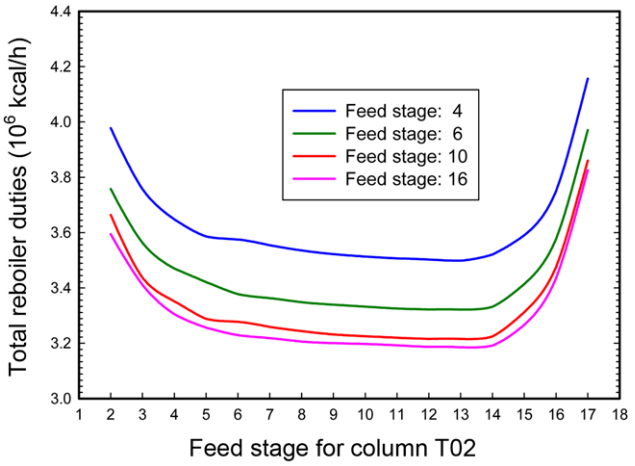

Fig. 7. Optimal feed stage location that minimizes the total reboiler heat duty.

Table 6. Determination of the THF recovery column feed stage location that minimizes the total reboiler heat duty

Case	T01 column feed stage	Optimal feed stage to T02	Total reboiler heat duties (10^6 kJ/h)
1	4	13	14.3511
2	6	13	13.6021
5	10	13	13.1692
6	16	13	13.0355

ing pressure of the H_2O removal column was atmospheric pressure. The type of condenser was a sub-cooled condenser and the type of internal column was set as a valve tray. The purity of water at the bottom column was fixed to 99.9 mole%. The operating pressure of the second THF recovery column was 7 bar, and the type of condenser was a sub-cooled condenser, and the type of column internal was considered as a valve tray. The purity of the THF in the bottom column was fixed to 99.9 mole%.

Fig. 6 shows that the total reboiler heat duties as a function of recycle flow rate of the THF recovery column top stream when the reflux ratio of the H_2O removal column is increased from 0.1 to 0.6. According to Fig. 6, the global minimum for the PSD process corresponds to case 4. When the reflux ratio of the H_2O removal column is decreased from 0.1 to 0.4, the local minimum for the total reboiler heat duties has a lower value. Table 5 shows each local minimum values for the total reboiler heat duties as a function of the reflux ratio for the H_2O removal column and the recycle flow rate for the THF recovery column top stream. According to Table 5, the global minimum point for the total reboiler heat duties is 13.7209×10^6 kJ/h when the recycle flow rate for the THF recovery column top stream is 5,072.5 kg/h.

Finally, the total reboiler heat duty was minimized by changing the feed stage location of the THF recovery column when the feeding stage to the H_2O removal column was 4, 6, 10 and 16 as shown in Fig. 7. Table 6 shows each local minimum values for the total reboiler heat duty as a function of the feed stage location for the THF recovery removal column when the feed stage to the H_2O removal column was 4, 6, 10 and 16. As shown in Table 6, the global minimum point for the total reboiler heat duty was 13.0355×10^6 kJ/h when the feed stage to the H_2O removal column was 16 and the feeding stage to the THF recovery column was 13. Compared to the total reboiler heat duty, 13.0355×10^6 kJ/h was found to be the

Table 7. Summary of column simulation results

Column		H_2O removal column	THF recovery column
Reflux ratio		0.4	0.4
Reflux molar rate (kmol/h)		54.9	34.9
Feed stage location from top		16	13
Condenser duty (10^6 kJ/h)		−6.8363	−5.0714
Cooling water consumption (ton/h)		204.2	151.5
Column top temperature (°C)		69.4	135.4
Reboiler duty (10^6 kJ/h)		7.2981	5.7374
Column bottom temperature (°C)		97.9	144.1
Reboiler return temperature (°C)		108.6	144.3
Steam consumption (kg/h)		3,629	2,853
Column diameter (mm)	Top	1,067	762
	Bottom	1,219	914
Flooding percent (%)		80	80
Tray spacing (mm)		610	610
Column efficiency (%)		54	60

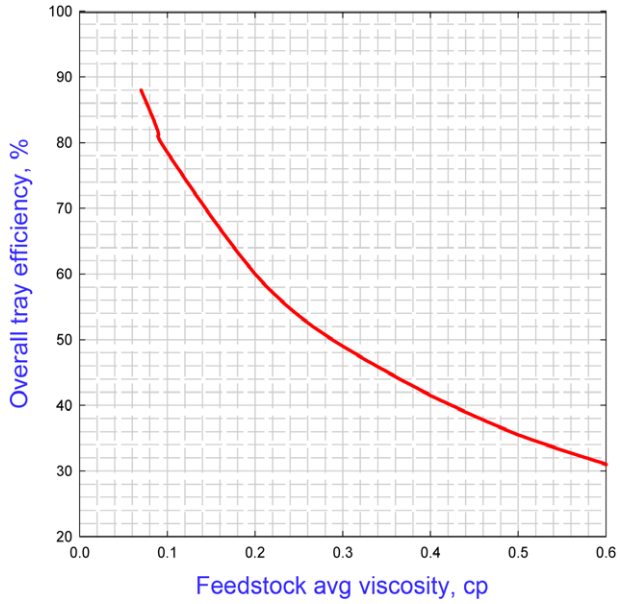

Fig. 8. Overall tray efficiencies as a function of feedstock average liquid viscosity.

global minimum point. As shown in Table 5, the total reboiler heat duty decreased by 4.02%. For the feed stage location above 16 for the H_2O removal column, there was no converged solution.

Table 7 summarizes the result of the simulation and optimization for the PSD separation process. To minimize the total reboiler duty, the reflux ratio of the first column was set to 0.4, the feeding stage location was at the 16^{th} stage, the heat duty of the condenser was -6.8363×10^6 kJ/h, the heat duty of the reboiler was 7.2981×10^6 kJ/h, the cooling water consumption was 204.2 ton/h, and the steam consumption was 3,629 kg/h. On the other hand, the total heat duty of the reboilers was at its minimum when the reflux ratio of the second column was 0.4 and the feed stage was at the 13^{th} stage. In this case, the heat duty of condenser was -5.0714×10^6 kJ/h, the heat duty of the reboiler was 5.7374×10^6 kJ/h, the cooling water consumption was 151.5 ton/h, and the steam consumption was 2,853 kg/h. The diameter of the each column was sized when the flooding percent was 80%. The diameter of the top section of the first column was 1,067 mm and the bottom section was 1,219 mm. The top section of the second column was 762 mm and the bottom section was 914 mm.

To estimate the efficiency of the distillation column, as shown in Fig. 8, the tray efficiency was estimated as a function of viscosity at the average temperature of the liquid phase stream feeding to the column. As shown in Fig. 8, since the average viscosity of the first column was 0.32 cP, the efficiency of the stage was 47%. Simi-

Table 8. Heat and material balance for pressure swing distillation process

Stream number	1		2		3		4	
Stream name	Feed		Overall feed		T01 top		T01 bottom	
Component	kmol/h	mole%	kmol/h	mole%	kmol/h	mole%	kmol/h	mole%
THF	50.00	50.00	108.75	58.04	108.70	79.17	0.05	0.10
H2O	50.00	50.00	78.61	41.96	28.60	20.83	50.02	99.90
Flowrate (kmol/h)	100.00	100.00	187.36	100.00	187.30	100.00	50.07	100.00
Temperature (°C)	25.0		34.9		45.0		108.6	
Pressure (bar)	2.50		2.00		1.05		1.40	
Stream number	5		6		7		8	
Stream name	Feed to T02		T02 top		T02 bottom		Recycle to T01	
Component	kmol/h	mole%	kmol/h	mole%	kmol/h	mole%	kmol/h	mole%
THF	108.70	79.17	58.64	67.26	50.06	99.90	58.64	67.26
H2O	28.60	20.83	28.55	32.74	0.05	0.10	28.55	32.74
Flowrate (kmol/h)	137.30	100.00	87.18	100.00	50.11	100.00	87.18	100.00
Temperature (°C)	45.4		45.0		144.3		45.0	
Pressure (bar)	8.00		7.00		7.40		2.00	

larly, since the average viscosity of the second column is 0.18, the efficiency of the stage was 63%.

The heat and material balance results are summarized in Table 8. As shown in Table 8, the purity of the water at the bottom of the first column was 99.9 mole%, the purity of THF at the bottom of the second column was 99.9 mole% and the recovery ratio of THF for the feed was 99.9%.

CONCLUSIONS

We have completed the simulation and optimization work for the PSD process between THD and water system by using a Wilson liquid activity coefficient model having binary adjustable parameters. Through this study, we presented the process engineering results for the basic and detail engineering to obtain a purified THD product from water through PSD process using a general purpose simulator, PRO/II with PROVISION release 8.3.

NOMENCLATURE

T : absolute temperature [K]
P : pressure [bar]
R : gas constant [J/gmole-K]
N : number of components
v : molar volume [m^3/gmole]
x_i and y_i : liquid and vapor phase mole fraction of component i and j
$\hat{f}_i^{vap}$: vapor phase fugacity coefficient of component i in a mixture
γ_i : activity coefficient of component i
P_i^{vap} : vapor pressure of component i
a_{ij} and A_{ij} : binary interaction parameters in Wilson model
a_c : energy parameter in Peng-Robinson equation
b : size parameter in Peng-Robinson equation
α : alpha function in Peng-Robinson equation
v_i^L and V_j^L : liquid molar volume in Wilson model
T_i^{exp} and T_i^{cal} : experimental and calculated dew point temperature

REFERENCES

1. R. H. Perry and D. W. Green, *Perry's Chemical Engineers' Handbook*, McGraw-Hill, New York (1997).
2. J. P. Knapp and M. F. Doherty, *Ind. Eng. Chem. Res*., **31**, 346 (1992).
3. H. E. Roscoe and W. Dittmar, *J. Chem. Soc*., **12**, 128 (1859).
4. H. E. Roscoe, *J. Chem. Soc.*, **13**, 146 (1860).
5. W. K. Lewis, US Patent, 1,676,700, July 10 (1928).
6. J. Gmehling and R. Boelts, *J. Chem. Eng. Data*, **41**, 202 (1996).
7. Repke et al., *Chem. Eng. Res. Design*, **85**, 492 (2007).
8. A. Klein and J.-U. Repke, *Asia-Pac. J. Chem. Eng*., **4**, 893 (2009).
9. G. Modla and P. Lang, *Chem. Eng. Sci.*, **63**, 2856 (2008).
10. Modla et al., *Chem. Eng. Sci*, **65**, 870 (2010).
11. Modla and Lang, *Ind. Eng. Chem. Res*., **49**, 3785 (2010).
12. W. L. Luyben, *Ind. Eng. Chem. Res*., **44**, 5715 (2005).
13. W. L. Luyben, *Ind. Eng. Chem. Res*., **47**, 2696 (2008).
14. W. L. Luyben, *Ind. Eng. Chem. Res*., **47**, 2681 (2008).
15. J. R. Phimister and W. D. Seider, *Ind. Eng. Chem. Res.*, **39**, 122 (2000).
16. S. Ray, N. R. Singha and S. K. Ray, *Chem. Eng. J.*, **149**, 153 (2009).
17. J. H. Cho, J. K. Park and J. K. Jeon, *J. Ind. Eng. Chem.*, **12**(2), 206 (2006).
18. J. H. Cho and J. K. Jeon, *Korean J. Chem. Eng.*, **23**(1), 1 (2006).
19. G. Soave, *Chem. Eng. Sci.*, **35**, 1197 (1972).
20. D. Y. Peng and D. B. Robinson, *Ind. Eng. Chem. Fundam.*, **15**, 58 (1976).
21. M. H. Holmes and M. van Winkle, *Ind. Eng. Chem.*, **62**(1), 21 (1970).
22. R. V. Orye and J. M. Prausnitz, *Ind. Eng. Chem.*, **57**(5), 18 (1965).
23. G. M. Wilson, *J. Amer. Chem. Soc.*, **86**, 127 (1964).
24. H. Renon and J. M. Prausnitz, *J. Amer. Chem. Soc.*, **14**, 135 (1968).
25. J. A. Nelder and J. D. Mead, *Comput. J.*, **7**, 308 (1965).
26. R. Munoz, J. B. Monton, M. C. Burguet and J. de la Torre, *Sep. Pur. Technol.*, **50**, 175 (2006).